# Study on Capability of the Octocopter Configuration in a Finite Element Analysis Simulation Environment

MATHEW BABY, Benil, SHPANIN, Leonid <http://orcid.org/0000-0002-3085-4678> and ABRAMIUK, Misko

World Academy of Science, Engineering and Technology
International Journal of Mechanical and Mechatronics Engineering
Vol:19, No:3, 2025

# Study on the Capability of Octocopter Configuration in a Finite Element Analysis Simulation Environment

Benil Mathew Baby, Leonid Shpanin, Misko Abramiuk



***Abstract*—**In this paper, a mechanical structure is proposed for generating 100,000 volts on board the drone heavy-lift octocopter UAV (Unmanned Aerial Vehicle) and for exploring the possibility of using this structure to transfer the harvested energy wirelessly to nearby UAVs. The feasibility of generating of a large electric field around the UAV structure is investigated theoretically using ANSYS and MATLAB simulation tools. The high-voltage generation mechanism is based on the boost DC-to-DC conversion technique, utilizing a traditional voltage step-up converter and voltage multiplier circuits. The analysis of the modeled octocopter geometry and the corresponding electric field distribution around the vehicle is presented through graphical representation of the simulated parameters. Additionally, the use of traditional carbon fiber material in the proposed octocopter structure and its impact on the generated electric field is carefully considered.

***Keywords*—**High voltage production, energy harvesting, object modeling and control, unmanned aerial vehicle.

## I. Introduction

THE high-voltage energy harvesting on board of the UAV is one of the rapidly-growing emerging technologies with diverse applications in aerospace. Various energy harvesting and production techniques have already been investigated in multirotor drones, where energy is collected from the surrounding ambient environment and typically involves the conversion of solar, kinetic, or thermal energies into electrical energy [1]-[3]. Studies have investigated the use of piezoelectric energy harvesters for both low and high rotary motion applications, demonstrating that piezoelectric materials can be successfully integrated into piezoelectric energy harvester structures [4]-[7]. Energy systems, capable of operating at high-voltage on UAVs, enable a range of capabilities, such as electrostatic spraying for agriculture, dust and particle collection for environmental monitoring, and the operation of electrostatic sensors or actuators. These systems typically employ equipment, such as DC-to-DC boost converters and Cockcroft-Walton voltage multipliers with the purpose of achieving high efficiency amplification of low input voltages [8], [9].

In this paper, a UAV structure is proposed to generate 100,000 volts for production of a strong electric field on board of the UAV. The feasibility of using multirotor drone geometry to produce high voltage on board the UAV is investigated theoretically using ANSYS Maxwell [10] and MATLAB [11] Finite Element Analysis (FEA) simulation tools. For this study, the industrially manufactured MANTIS X8-PRO octocopter frame–a close equivalent to the TAROT X8-Lite octocopter frame [12]–was used to explore the octocopter operation which was modeled for simulation studies. The high-voltage components were developed by integrating mechanical parts into the octocopter geometry for simulation and analysis.

## II. Modeling of the Octocopter Energy Harvester

The lightweight aerial platforms have established the use of Cockcroft-Walton voltage multipliers combined with DC-to-DC boost converters to achieve scalable voltage amplification [8]. The method's compact design and high efficiency in generating high voltages with minimal weight addition make it well-suited for UAV applications [9]. Simulation-driven approaches using FEA tools such as MATLAB [11] and ANSYS Maxwell [10], have also been successfully employed to evaluate the UAVs electric circuit performance [13]. In this study, we evaluate an approach of generating a strong electric field around the UAV by integrating a metallic (stainless steel) sphere in the MANTIS X8-PRO octocopter frame [12]. The feasibility of producing a strong electric field was assessed by applying 100 kV to the surface of the metallic sphere in the ANSYS Maxwell simulation environment. Additionally, MATLAB simulations were conducted to evaluate the potential for high-voltage production on board the investigated octocopter structure.

### *A. Octocopter Conceptual Model*

The conceptual design involves integrating the MANTIS X8-PRO octocopter frame with a 22.2 V, 5300 mAh LiPo battery, along with electronic circuit, motors, and propellers positioned outside the metallic sphere. The arrangement is shown in Figs. 1 (a) and (b).

The total mass of the investigated multi-rotor octocopter structure, including the carbon fiber propellers, metallic sphere, and onboard electric and electronic circuits, is approximately 7 kg. This mass is within the lifting capacity of the MANTIS X8-PRO octocopter frame, which can support a total flying weight of up to 10 kg.

B. Mathew Baby, L. Shpanin, and M. Abramiuk are with the School of Engineering and Built Environment, Sheffield Hallam University, Sheffield, S1 1WB, UK (e-mail: benil.mathewbaby@student.shu.ac.uk, l.shpanin@shu.ac.uk, m.m.abramiuk @shu.ac.uk).

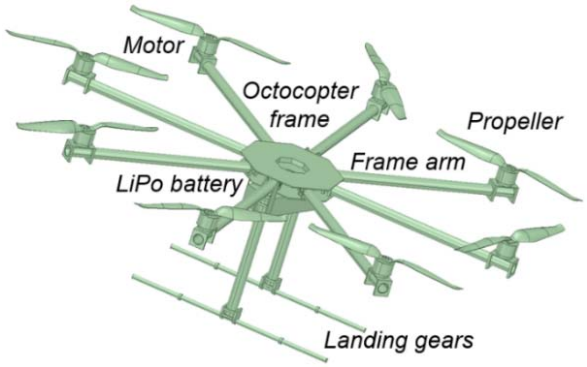


(a)

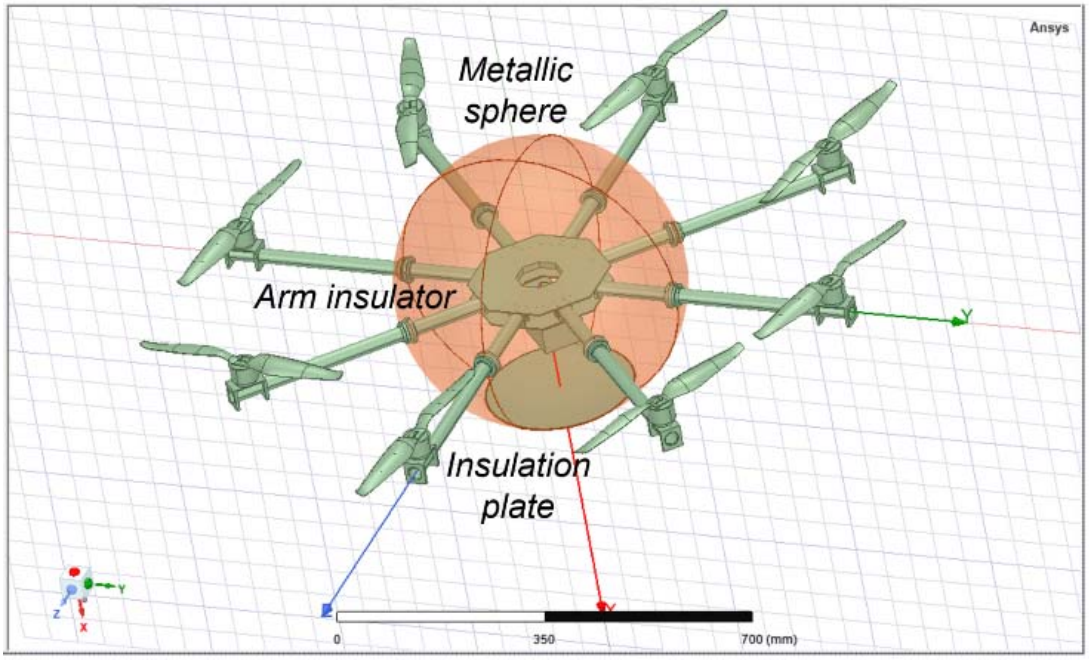


(b)

Fig. 1 Conceptual design of the octocopter with integrated metallic sphere of 500 mm diameter and thickness of 1 mm: (a) Octocopter modeled structure with the landings gears, (b) Octocopter modeled structure (without the landing gears) integrated with metallic sphere in ANSYS Maxwell (Electromagnetics simulation software)

### *B. ANSYS Maxwell and MATLAB Simulation Setup*

The study of the electric field distribution around the metallic spherical conductor (made of stainless-steel material) was conducted using ANSYS 3D Maxwell Electronics Desktop, an electromagnetic simulation software [10]. The modeled structure, shown in Fig. 1 (b), was simulated in atmospheric-pressure air, used as the background in the simulation setup. A voltage of 100 kV was applied to the metallic sphere to analyze the electric field behavior. ANSYS 3D Maxwell utilizes Maxwell's equations to solve for electric field parameters within an environmental volume of approximately 2 square meters. Mesh refinement and appropriate boundary conditions were set to ensure accurate representation of the electric field intensity. The electric field (E), measured in volts per meter [V/m], was calculated through the electric flux density and vector parameters using the electrostatic solver. The solver employs automatic adaptive meshing to refine the mesh and enhance the accuracy of the simulation results.

## III. Simulation Results and Analysis

### *A. ANSYS Maxwell Electric Field Simulation Results*

The electric field distribution around the modeled octocopter and metallic sphere (containing the LiPo battery, electric, and electronic circuits) is shown in Figs. 2 (a) and (b) and 3 (a)-(c). The electric field intensity is visualized using a color gradient, where green, yellow, and red indicate regions of higher field strength, particularly near the surface of the metallic sphere and propellers. The intensity decreases as the distance from the metallic sphere increases, with the blue gradient representing areas of lower field strength.

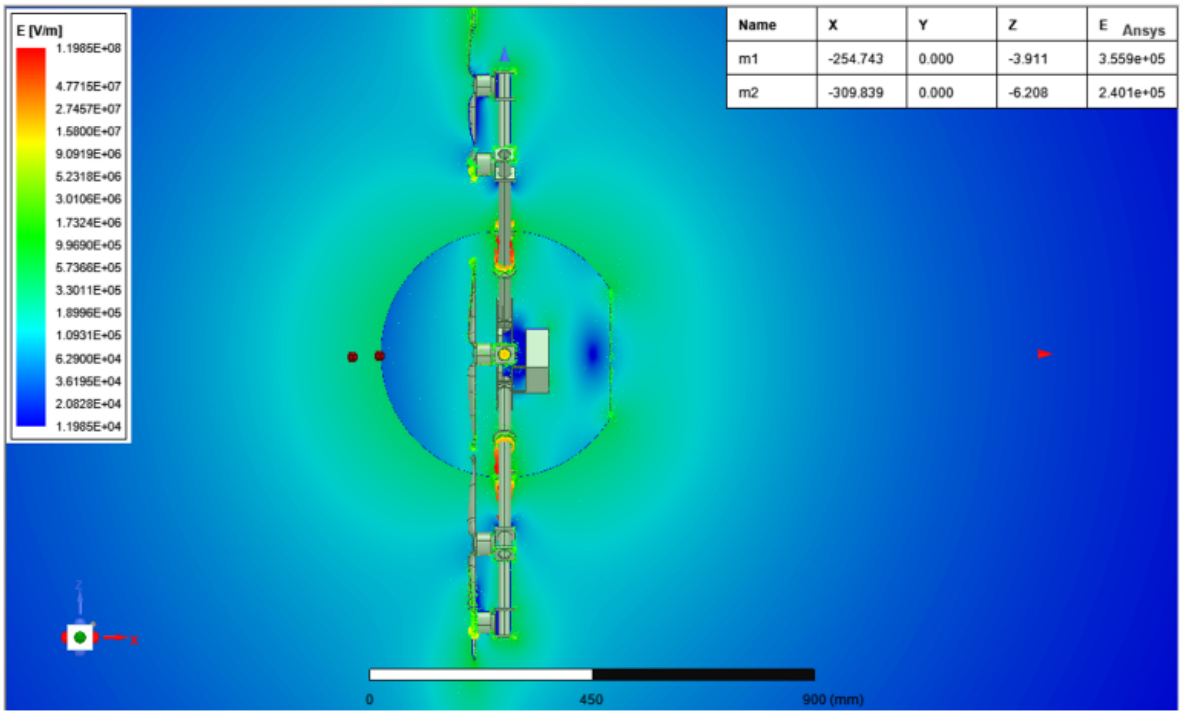


(a)

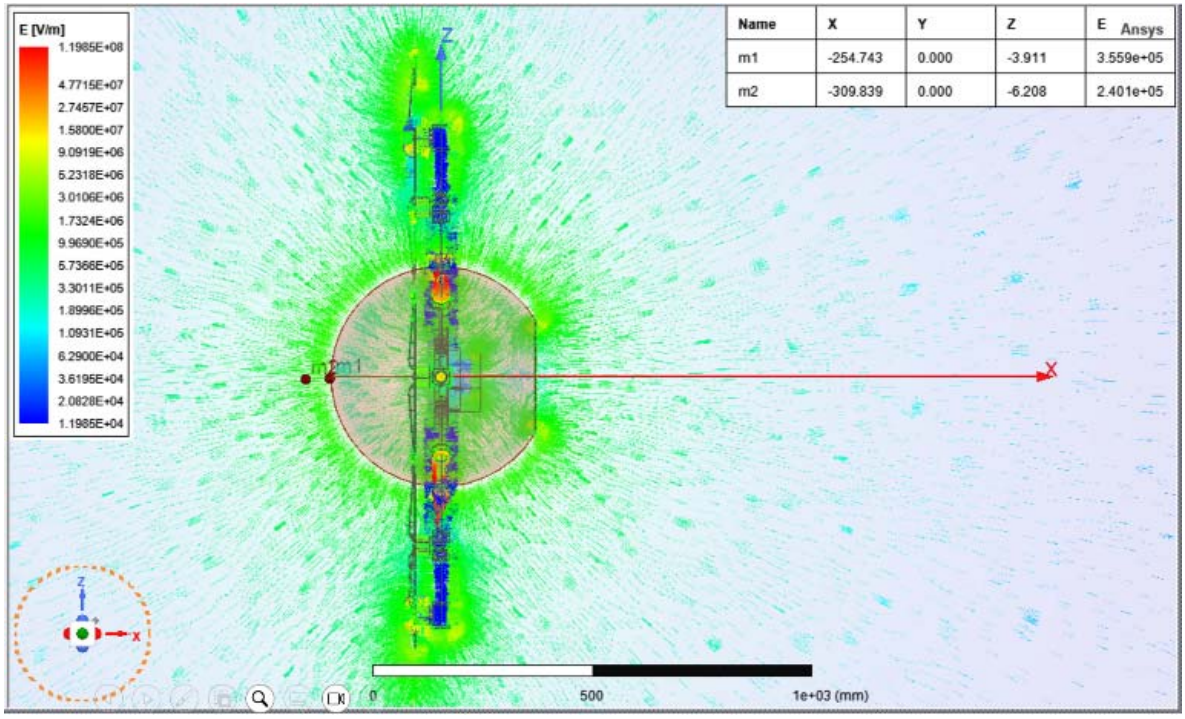


(b)

Fig. 2 ANSYS Maxwell simulation results of the octocopter with metallic sphere structure shown as zx-plane cross-sectional view: (a) Electric flux density distribution, (b) Electric field vector direction.

Fig. 2 (a) illustrates a surface plot of the electric field distribution pattern on the metallic sphere surface. The simulation results indicate that the electric field strength magnitude at distance of 55 mm from the metallic sphere is $2.401 \times 10^5$ V/m as shown from (point: m2). Fig. 2 (b) shows the electric field vector distribution around the metallic sphere, revealing that the field is outward of the metallic sphere. The electric field is concentrated near the edges of the metallic

sphere, with its direction extending from interior of the sphere to the surrounding environment. The highest concentration of the electric field is observed around the edges of the metallic sphere cut as it has sharp edges. The red and yellow colors indicate the high concentration of electric flux density around the sphere cut and the holes created for inserting the octocopter arms through the arm insulators into the sphere.

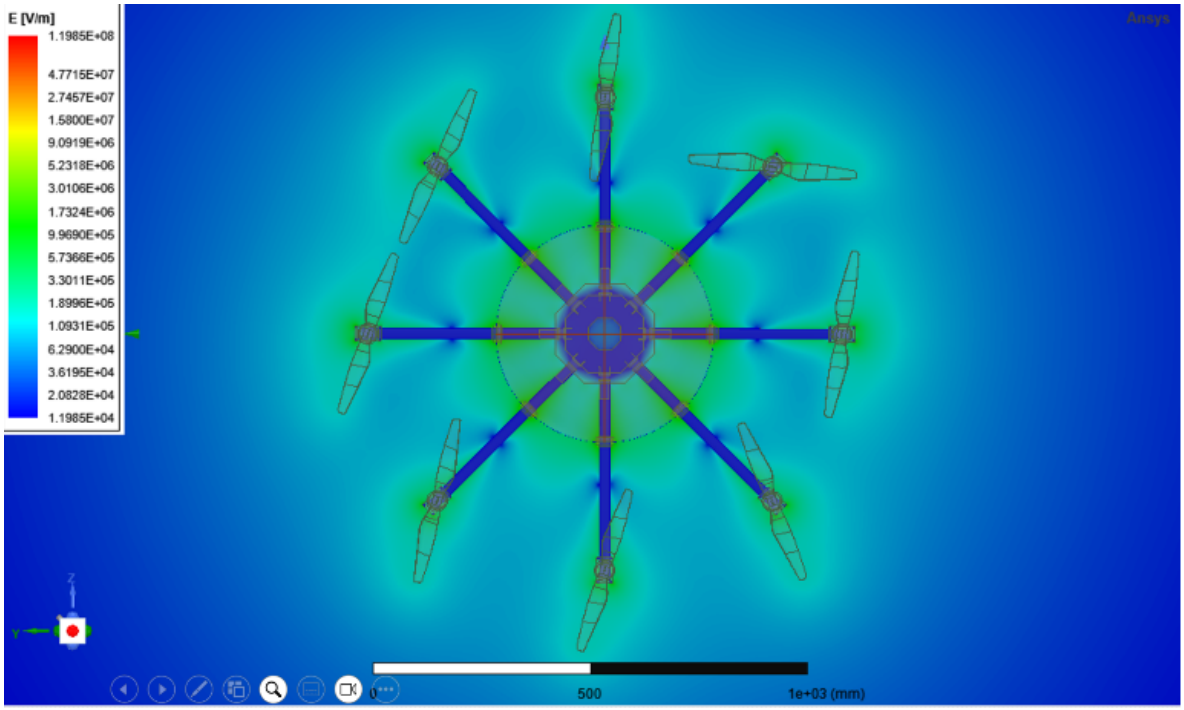


(a)

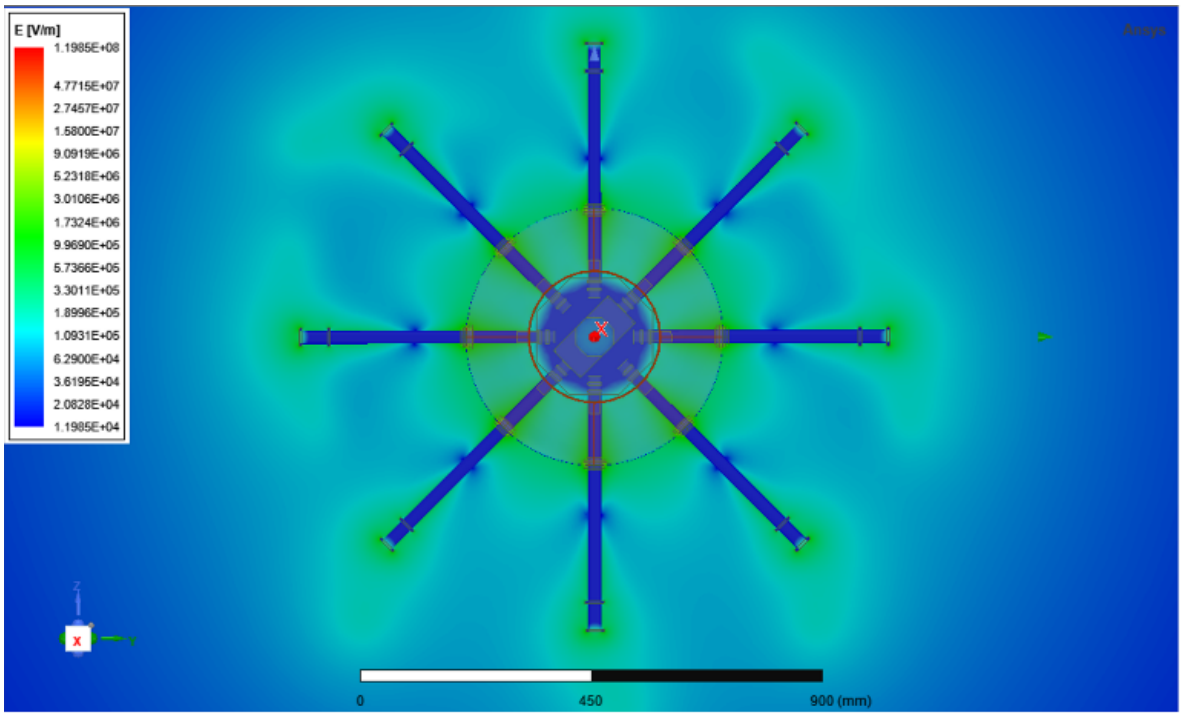


(b)

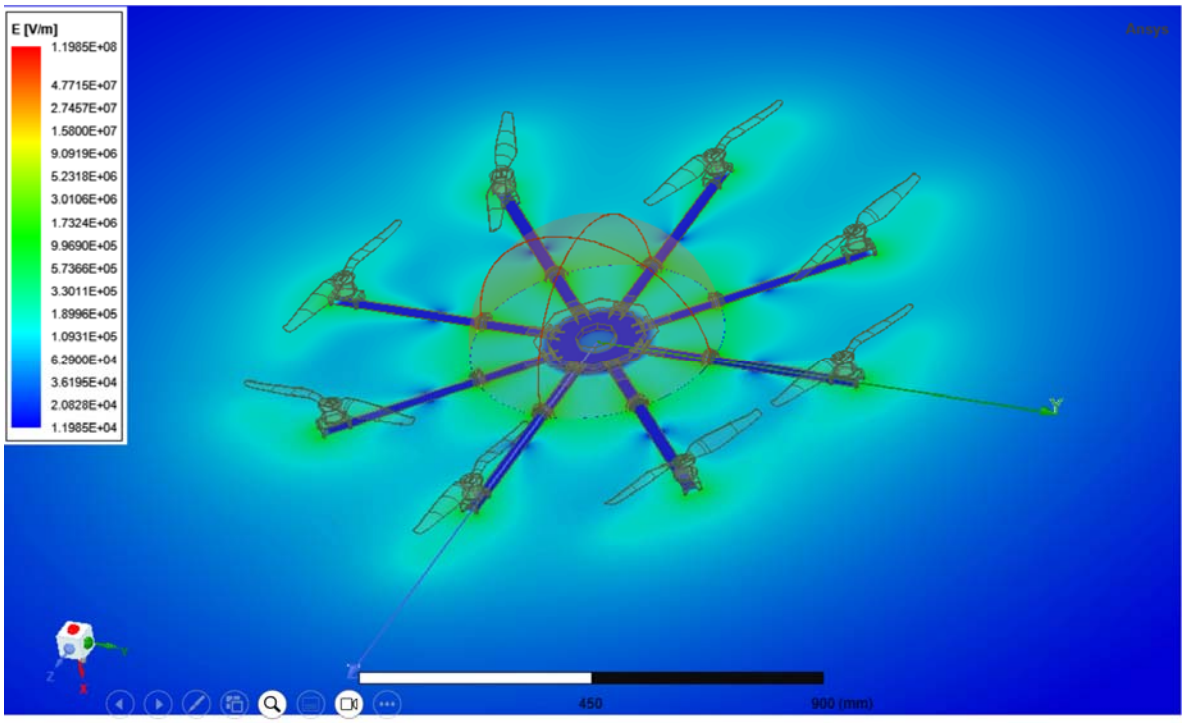


(c)

Fig. 3 ANSYS Maxwell simulation results of the octocopter with metallic sphere structure at different positions in space: (a) Top view of the structure, zy-plane cross-sectional view, (b) Bottom view of the structure, zy-plane cross-sectional view, (c) 3D Top view of the structure, zy-plane cross-sectional view

Figs. 3 (a)-(c) present the ANSYS 3D Maxwell results in the zy-plane cross-sectional view. The results reveal a non-uniform electric flux density distribution around the metallic sphere, particularly at the top and bottom sections of the octocopter structure (Figs. 3 (a), (b)). High electric flux concentration is observed near to the motors and propellers of the octocopter structure, likely due to the use of carbon fiber material in octocopter arms and propellers, which may facilitate charge transfer from the metallic sphere along their surfaces.

*B. MATLAB DC-DC Boost Converter and Voltage Multiplier Simulation Results*

The boost converter, a type of switch mode converter, is designed to step up the relatively low input voltage from a 22.2 V LiPo battery to a significantly higher output voltage. It operates by alternately storing and releasing energy through the inductor, capacitor, and load resistor components [8], [9]. In this set up, an inductor of 1mH, a capacitor of 1 μF, and a load resistance of 50 Ω were used, with the switch duty cycle set at 0.95 for maximum voltage step-up. A switching frequency of 50 kHz and a time step at T/100 ensure accurate results.

The boost converter operates in two phases:

- *Switch-on phase:* The input supply charges the inductor.
- *Switch off phase:* The stored energy of inductor is released to the load through the capacitor.

Since the output voltage stabilizes to a higher value, we scale it to 10 kV and pass it through another Cockcroft - Walton voltage multiplier [9]. An example of the boost converter output voltage over time simulated in MATLAB is shown in Fig. 4. It shows that the voltage rises from 0 to some value near 5 kV with small ripples occurring on account of switching effects and dynamics of the capacitor charging.

A Cockcroft-Walton voltage multiplier is also used to gain further amplification of the high-voltage DC from the boost converter [9]. To step-up voltage, there are multiple stages of the capacitor and the diode that form a voltage multiplier. The number of stages of the simulation goes from 1 to 6 and load resistances of 1000 Ω, 5000 Ω and 10000 Ω are considered. The voltage gain for each stage is calculated using (1):

$$V_{out} = \frac{2n.V_{in}}{1+\frac{n}{fCR_L}} \quad (1)$$

where, $V_{in}$ is the input voltage, [V], $n$ is a number of stages, $f$ switching frequency, [Hz], C capacitance, [F] and $R_L$ is the load resistance [Ω]. Output voltage gain increases proportionally as the number of stages increases and is however limited by load resistance as well as component losses. The voltage gain per stage as a function of load resistances is shown in Fig. 5. From the results, we can see that a higher load resistance indicates a higher voltage gain. In fact, the maximum voltage gain is shown, which occurred with $R_L$ = 10000 [Ω] and six stages.

In addition, it is found that the load resistance connected to the voltage multiplier directly determines the final voltage amplification. As the load resistance increases, the final output voltage rises due to the reduce current drawn from the source, allowing the voltage to reach higher levels. Fig. 6 demonstrates

the relationship between the load resistance and final voltage amplification, as simulated in MATLAB.

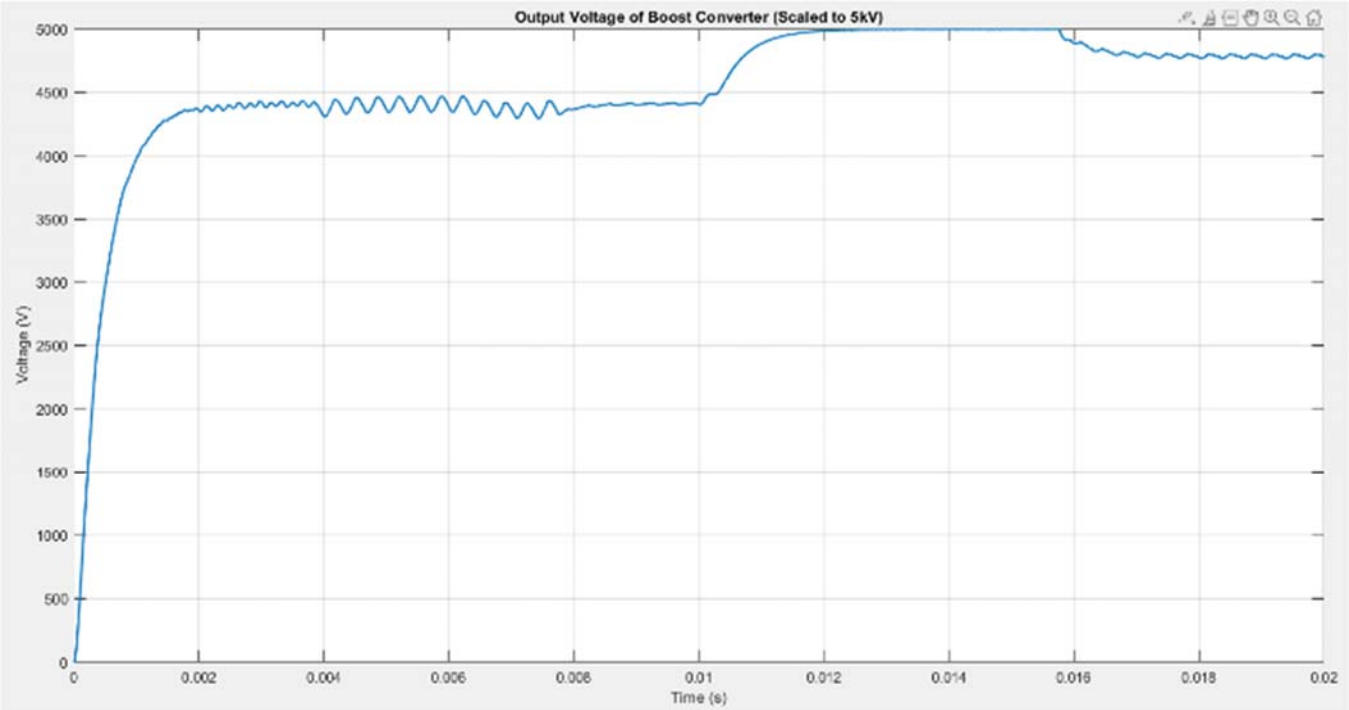


Fig. 4 Output voltage of the boost converter over time

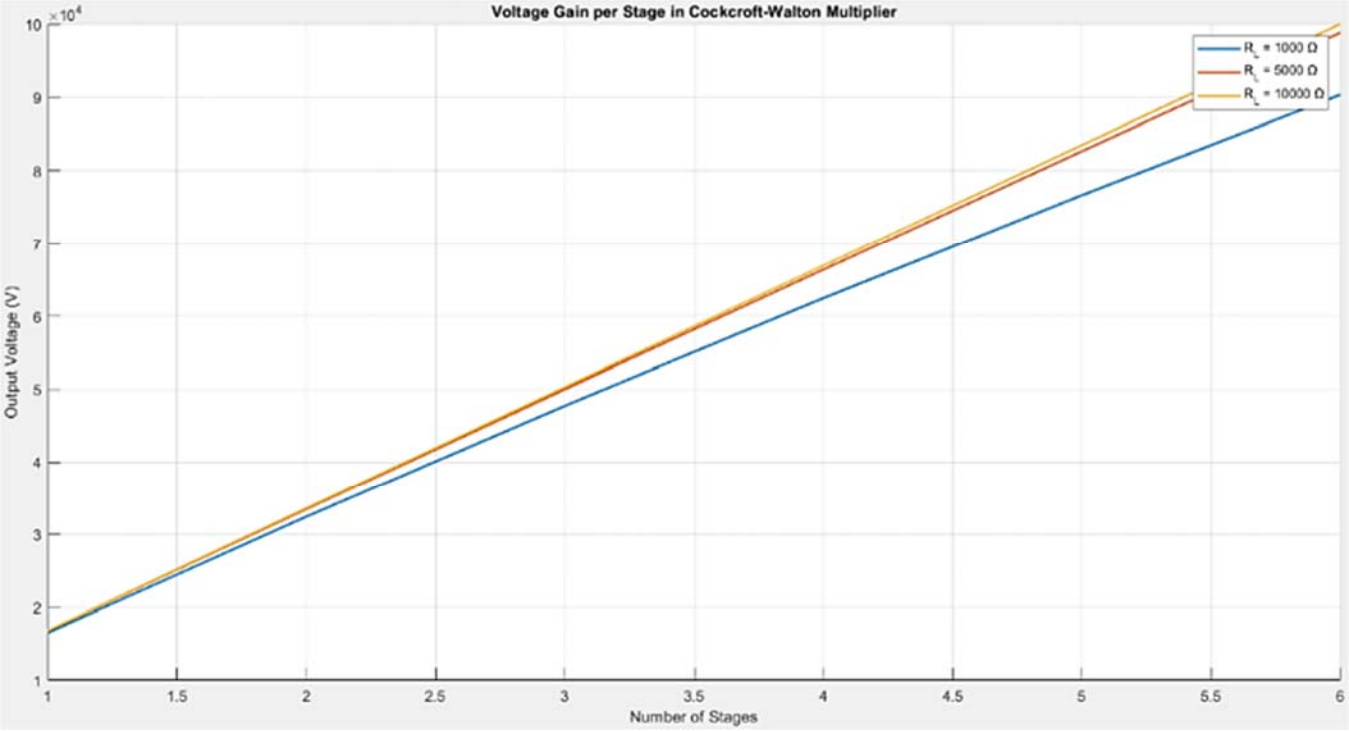


Fig. 5 The voltage gains of the multiplier per stage for different load resistances

The trend clearly shows that increasing the load resistance results in a higher voltage gain. As the load resistance approaches 10000 Ω, the voltage gain begins to plateau. In other words, this behavior characteristic of voltage multipliers, where minimizing the load current allows for maximizing the voltage gain.

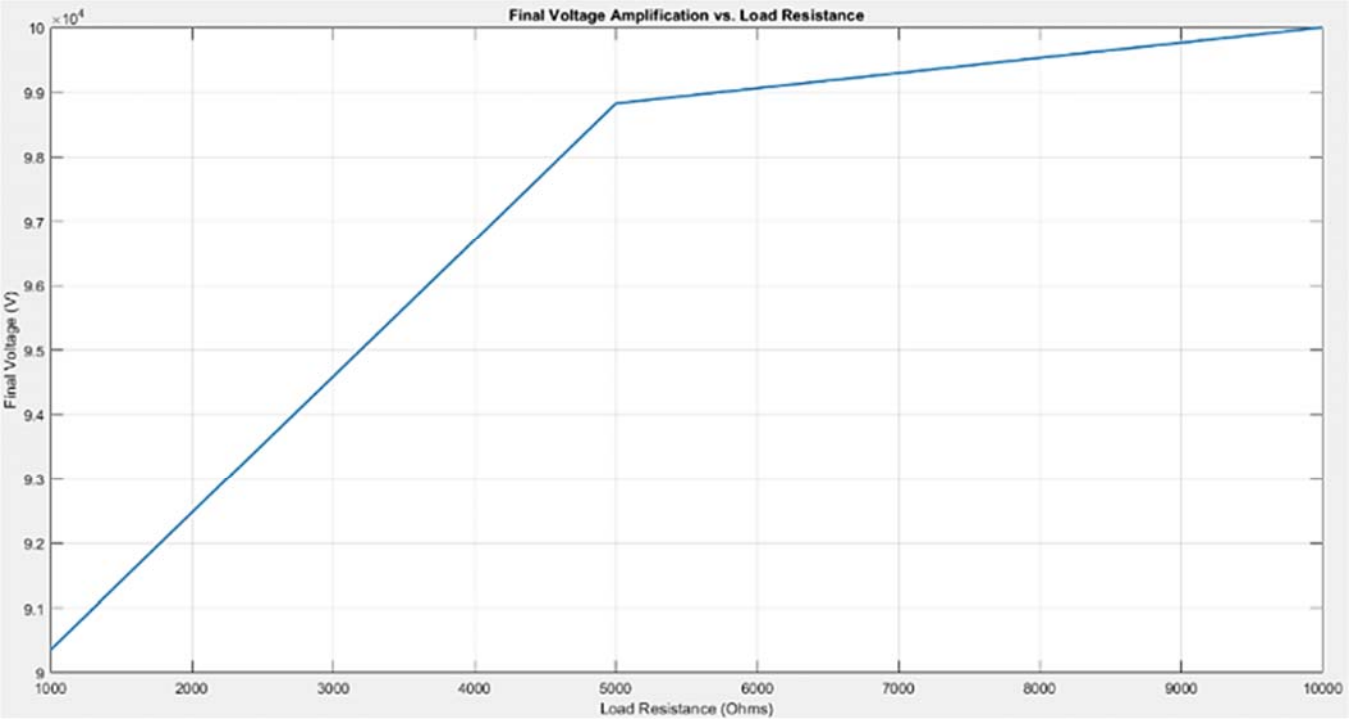


Fig. 6 The relationship between load resistance and final voltage amplification

## IV. Conclusions

The feasibility study of the integrated octocopter and metallic sphere structure for producing a strong electric field around the UAV was investigated in this paper. The primary objective of this work was to develop a 100 kV high-voltage energy production mechanism capable of generating a strong electric field on board the vehicle. A 22.2 V, 5300 mAh LiPo battery was used as the primary power source. The DC-DC boost converter was evaluated to provide a step-up voltage, while the Cockcroft-Walton voltage multiplier was investigated to provide further voltage amplification. ANSYS Maxwell and MATLAB simulations demonstrated that the proposed system can generate a strong high-voltage electric field which can be considered for different UAV applications including electrostatic spraying, dust mitigation, atmospheric particle collection, and the possibility of wirelessly transferring the harvested energy to nearby UAVs without using landing gear in the proposed octocopter configuration. The modularity of the proposed system allows for scalability across several types of UAV configurations, validating the viability of the proposed energy production system for real-world applications. Further experimental investigations of the proposed concept are needed to validate the proposed concept practically.

## Acknowledgment

The authors appreciate the support provided by Mr. Steven Brandon and Mr. Jeet Shende for their assistance in the CAD modeling work.

## References

[1] S. Cass, "Beyond the Quadcopter: New Designs for Drones Showcased at CeBIT", *IEEE Spectr.* 53 (5), pp.21-22, 2016.

[2] M. Shaheed, A. Abidali, J. Ahmed, S. Ahmed, I. Burba, P. Fani, G. Kwofie, K. Wojewoda and A. Munjiza, "Flying by the Sun only: The Solarcopter prototype" *Aerospace Science and Technology*, vol. 45, pp.209-214, 2015.

[3] J. Fleming, W. Ng and S. Ghamaty, "Thermoelectric-Based Power System for Unmanned-Air-Vehicle/ Microair-Vehicle Applications", *Journal of Aircraft*, 41(3), pp.674-676, 2004.

[4] N. Osuchukwu, L. Shpanin, "Feasibility Study of the Quadcopter Propeller Vibrations for the Energy Production", *International Journal of Mechanical, Aerospace, Industrial, Mechatronic and Manufacturing Engineering*, Vol. 11 No. 2: pp.277-283, Feb. 2017.

[5] L. Shpanin, M. Abramiuk, M. Goodwin, K. Bernard, A. Karuva Chalil, N. Osuchukwu, N. Pickett, "Smart Control of the Multirotor Drone Propeller for Enhanced Vibration Energy Harvesting", *IEEE Aerospace Conference*, Montana, USA, pp.1-11, May 2024. Available: http://doi.org/10.1109/AERO58975.2024.10520938

[6] F. Khameneifar, S. Arzanpour, and M. Moallem, "A piezoelectric energy harvester for rotary motion applications: Design and Experiments", *IEEE/ASME Transactions on Mechatronics*, vol. 18, (5), pp.1527-1534, 2013.

[7] S. Anton and D. Inman, "Vibration Energy Harvesting for Unmanned Aerial Vehicles", *Active and Passive Smart Structures and Integrated Systems*, vol. 6928 (24), 2, 2008.

[8] T. V. Quyen, C. V. Nguyen, A. M, Le, M. T. Nguyen, "Optimizing Hybrid Energy Harvesting Mechanisms for UAVs", *EAI Endorsed Transactions on Energy Web*, 164629, pp.1-8, 2018. Available: https://doi.org/10.4108/eai.13-7-2018.164629

[9] S. Park, D. S. Drew, S. Follmer, J. Rivas-Davila, "Lightweight High Voltage Generator for Untethered Electroadhesive Perching of Micro Air Vehicles", *IEEE Robotics and Automation Letters*, Vol. 5, (3), 4485–4492, 2020. Available: https://doi.org/10.1109/lra.2020.3001520

[10] ANSYS Maxwell Online. Available: https://www.ansys.com

[11] MATLAB Online. Available: https://www.mathworks.com

[12] TAROT X8-Lite Online. Available: https://www.flyingtech.co.uk/product/tarot-x8-lite-1050mm-foldable-octocopter-frame/

[13] Y. Yan, W. Shi, X. Zhang, "Design of UAV Wireless Power Transmission System Based on Coupling Coil Structure Optimization", *EURASIP Journal on Wireless Communications and Networking*, 2020. Available: https://doi.org/10.1186/s13638-020-01679-4